DOI: 10.1002/adma.200703159

Proton Conductivity Enhancement by Nanostructural Control of Poly(benzimidazole)-Phosphoric Acid Adducts**

By *Jens Weber, Klaus-Dieter Kreuer, Joachim Maier,* and *Arne Thomas**

Fuel cells are, in terms of economic and environmental concerns, an interesting alternative to existing power conversion systems because they combine high efficiency with the usage of fuels that have the potential to be renewable. Because of their low operating temperatures, polymer exchange membranes fuel cells (PEMFCs) are interesting for applications in transportation and portable electronics. To optimize the efficiency of the PEMFC, high demands are put on the polymer membrane, for example, a high conductivity should be ensured in a wide temperature window. Especially the design of proton-conducting membranes that are stable and provide good performance above $T = 100\,^{\circ}\mathrm{C}$ presents a major challenge.

One of the few materials that shows interesting properties in these respects are adducts of poly(benzimidazole) (PBI) and phosphoric acid (PA).[1–4] For high concentrations of PA such materials show high proton conductivity well above $T = 100\,^{\circ}\mathrm{C}$, and numerous fuel tests have provided promising results.[2–4] While perfluorosulfonic acid (PFSA) membranes such as Nafion exhibit high conductivity only when hydrated, PBI/H_3PO_4 systems display high conductivity even at low relative humidity. As for pure phosphoric acid,[5] the proton-conduction mechanism is of the structure diffusion type (Grotthuss mechanism), that is, protonic defects just follow the diffusion of structural patterns, which is brought about by some local dynamics but does not require any long-range transport (diffusion) of phosphate species.[6] This enables these membranes to operate at temperatures above $T = 80\,^{\circ}\mathrm{C}$; typically the limiting operating temperature for PFSA membranes. Higher operation temperatures are actually desired for a number of reasons including (i) enhanced activity of the electrocatalysts (especially for the oxygen reduction reaction), (ii) reduced sensitivity of the catalysts to contaminants, (iii) the absence of any liquid water management, and finally (iv) significantly improved head ejection.

It was also shown that proton conductivity in polymer membranes benefits from a biphasic structure, as it is found in hydrated sulfonated polymers (e.g., Nafion or sulfonated PEEK).[7] The biphasic structure with nanometer sized pores and channels supports proton transport, which takes place in a phase with a local liquid-like dynamics while the second (polymer) phase supports the mechanical stability of the system.

It is a common observation for PBI/H_3PO_4 systems that their conductivity strongly increases in a non-linear fashion with increasing amount of the oxo-acid and finally approaches the conductivity of the pure acid.[3,8] Some authors assumed that an excess acid doping of PBI leads to the formation of phosphoric acid domains, but there is only little experimental evidence for this assumption.[3]

Motivated by these observations, Mecerreyes et al. presented an approach towards porous PBI membranes, which enables high acid uptakes.[9] Macroporous membranes with porosities up to 75% were generated by leaching out a low-molecular-weight porogen. The resulting membranes showed an increased acid uptake and thus enhanced proton conductivity. However, as stated by the authors only ill-defined macropores were obtained, but the conductivity could still be tuned by the preceding porogen content. Recently, the synthesis of mesoporous PBI (mp-PBI) networks by a solvent-mediated hard-templating procedure was presented.[10] The resulting PBI networks had a defined pore size of about 10 nm and specific surface areas and porosities of up to $190\,\mathrm{m}^2\,\mathrm{g}^{-1}$ and 37 vol %, respectively (Fig. 1). It was shown that the porosity of these polymer networks could be easily tuned by the amount of the silica used as template and by the crosslinking density.

Herein we present the results of proton-conductivity measurements of this mesoporous PBIs filled with nominally dry phosphoric acid for temperatures up to $T = 180\,^{\circ}\mathrm{C}$.

As mentioned, for linear polymers a strong influence of the proton conductivity on the acid content is observed. At low filling levels the phosphoric acid protonates all imidazole nitrogen atoms, forming benzimidazolium cations and dihydrogenphosphate anions. For higher concentrations of phosphoric acid, the proton transfer is progressively taking place between phosphoric species, which leads to the

---

[*] Dr. A. Thomas, J. Weber
Department of Colloid Chemistry
Max-Planck-Institute of Colloids and Interfaces
Research Campus Golm, 14424 Potsdam (Germany)
E-mail: arne.thomas@mpikg.mpg.de
Dr. K.-D. Kreuer, Prof. J. Maier
Max-Planck-Institute for Solid State Research
Heisenbergstr. 1, 70569 Stuttgart (Germany)

[**] We gratefully acknowledge the help of Mrs. A. Fuchs with the preparation of the anhydrous crystalline phosphoric acid. M. Antonietti is acknowledged for fruitful discussions. Financial support from the ENERCHEM project of the MPS is acknowledged. Supporting Information is available online from Wiley InterScience or from the authors.

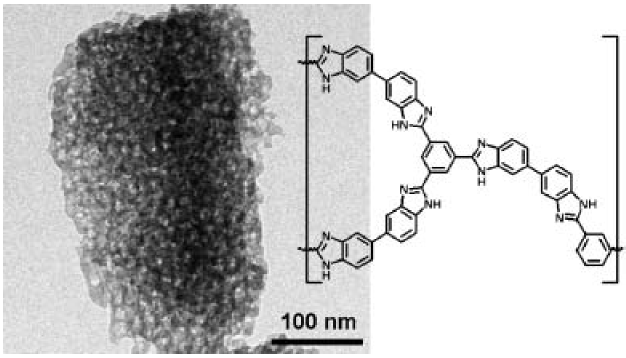

Figure 1. Transmission electron microscopy image of a mesoporous polybenzimidazole (mp-PBI) and schematic drawing of the chemical structure of the used polymer.

formation of mobile protonic defects and therefore to proton conductivity.[3]

Considering the distribution of phosphoric acid in mesoporous (mp) PBIs two situations may be envisaged: PA may either fill the mesopores and reduce the interfacial energy through capillarity or it may diffuse into the pore walls to bind chemically onto the benzimidazole moieties. To clarify this situation, samples with constant porosities were loaded with an amount of phosphoric acid matching the pore volume of the respective mp-PBI sample (a slight excess of PA of 3 wt % was used to ensure complete pore filling). Thus, for mp-PBI with a porosity of 29.5 vol %, a total mass of 40 wt % PA was added (mp-PBI/PA-40). For comparison, another sample of the same mp-PBI was loaded with an excess of phosphoric acid (mp-PBI/PA-66 for 66 wt % PA). Subsequently, the samples were heated to $T = 180\,^{\circ}\mathrm{C}$ for 12 h and then analyzed by nitrogen sorption and small-angle X-ray scattering (SAXS).

Figure 2 shows SAXS patterns of the described samples together with the SAXS pattern of a crosslinked, mesoporous PBI in its pure form.

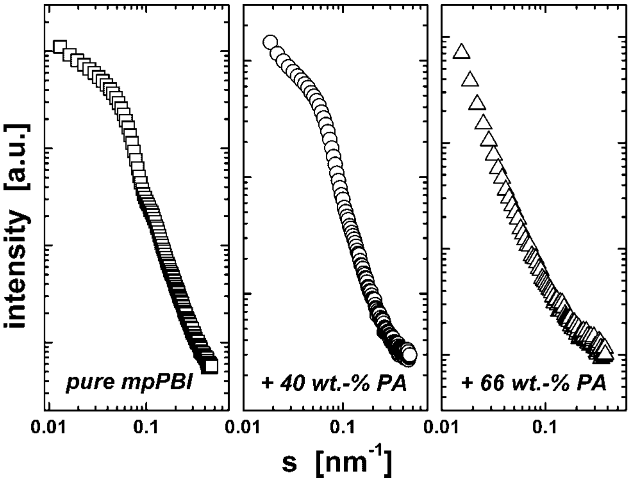

Figure 2. SAXS patterns of mesoporous PBI (left), mpPBI/PA-40 (middle) and mpPBI/PA-66, both after annealing (right).

The pure sample shows a scattering pattern typical for a material with disordered spherical mesopores.[10] For mp-PBI/PA-40 the scattering pattern also shows features characteristic for spherical scattering objects; however, the pattern is less defined compared to the pure mp-PBI sample. At higher filling levels (mp-PBI/PA-66) no scattering texture is visible anymore. Considering the small scattering contrast of PBI and phosphoric acid, that is, the small electron density difference, the evolution of the spectrum suggests some remaining porosity for mp-PBI/PA-40 and complete pore filling only for mp-PBI/PA-66. This implies incorporation of phosphoric acid also into the pore walls, which further reduces the scattering contrast.

This understanding is actually confirmed by the results of nitrogen sorption measurements. As expected, mp-PBI/PA-66 did not show any porosity, in accordance with the complete filling of the mesopores. In contrast, mp-PBI/PA-40 shows a defined porosity with a Brunauer–Emmett–Teller (BET) surface area of $25\,\mathrm{m}^2\,\mathrm{g}^{-1}$ and a hysteresis indicating the presence of mesopores. Barrett–Joyner–Halenda (BJH) analysis showed that the maximum of the pore size distribution is around 10 nm, which is exactly the size of the mesopores in the pure mp-PBI sample. However, the pore size distribution also showed the presence of smaller pores (Fig. S1).

Based on these observations, it may be assumed that the mesopores of mp-PBI are filled in a fast process owing to capillarity upon loading with molten phosphoric acid. However, in a second, slower step the phosphoric acid is diffusing into the pore walls to react with the benzimidazole moieties. In the case of adding a phosphoric acid volume matching the pore volume (mp-PBI/PA-40) the pores are partially emptied during this process. In contrast, an excess loading (mp-PBI/PA-66) ensures that the mesopores remain loaded throughout the penetration of the pore walls. It can be calculated that the amount of PA incorporated in the pore walls roughly equals the molar amount of benzimidazole moieties, as 66 wt % PA corresponds to 3 equivalents PA per benzimidazole unit. The overall process is depicted in Scheme 1.

The picture is confirmed by proton conductivity measurements performed on both samples before and after annealing at $T = 180\,^{\circ}\mathrm{C}$ for 12 h. All conductivity measurements were performed on nominally dry samples in closed cells. For mp-PBI/PA-40 a drop in conductivity from $1.8 \times 10^{-4}\ \mathrm{S \cdot cm^{-1}}$ to $0.4 \times 10^{-4}\ \mathrm{S \cdot cm^{-1}}$ is observed during annealing at $T = 180\,^{\circ}\mathrm{C}$. In contrast, mp-PBI/PA-66 showed a much higher conductivity with a lower relative decrease during annealing from $6.3 \times 10^{-3}\ \mathrm{S \cdot cm^{-1}}$ to $5.9 \times 10^{-3}\ \mathrm{S \cdot cm^{-1}}$. The huge difference in the proton conductivity observed for mp-PBI/PA-40 and mp-PBI/PA-66 can be explained by missing percolation of phosphoric acid domains in the case of the lower loading.

To evaluate the influence of the porosity on the proton conductivity, compressed pellets of a non-porous, but cross-linked PBI were prepared for comparison. Both samples then contained 20 mol % cross-linker (1,3,5-triphenyl mesitylate)[10] with respect to the 3,3′-diaminobenzidine. These two samples,

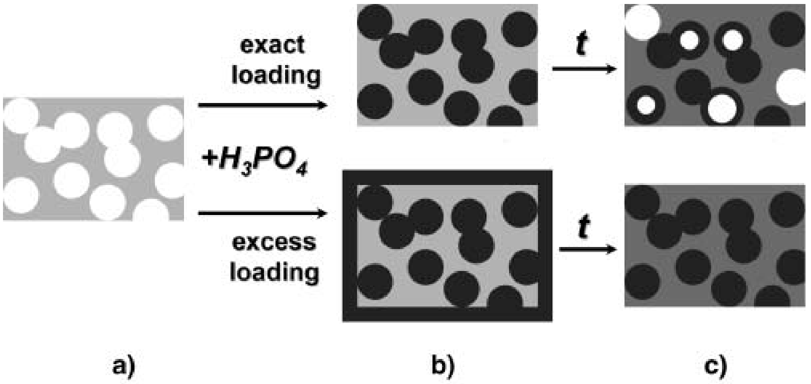

Scheme 1. "Two-step" loading of phosphoric acid in mesoporous PBI: First, the mesopores of mp-PBI (a) are loaded with PA due to capillarity (b), and second, PA gets incorporated into the pore walls (c).

the mesoporous and the non-porous PBI were both loaded with 66 wt % PA (mp-PBI/PA-66 and PBI/PA-66). It should be noted that the resulting samples therefore only differ in the nanostructure of the PBI membranes, while all other factors influencing the proton conductivity were held constant. The conductivity was measured after annealing the samples for 12 h at 180 °C. Figure 3 shows the measured conductivities in an Arrhenius plot.

The conductivity of the nanostructured material, mp-PBI/PA-66, is one to two orders of magnitude higher than that of nonporous PBI (PBI/PA-66). This observation clearly demonstrates the benefit of a biphasic structure of PBI/PA on the proton conductivity. Considering the highly nonlinear increase of the proton conductivity of "homogeneous" PBI/PA,[3,8,11] this is expected provided the highly conducting PA-rich domain is well connected. If this were not the case, an even lower conductivity than for nonporous PBI/PA is expected, because the total resistance is then mainly determined by the very high resistance of the PA-poor domain.

The results also prove that the nanostructural features are maintained after the annealing process, that is, no complete homogenization of the composites takes place. Also the high proton conductivities observed for mp-PBI/PA-66 can not be attributed to phosphoric acid located in interparticle voids of the pellets, as this would lead to similar conductivities for both samples.

It should be noted that the proton conductivity for the nonporous but crosslinked sample is significantly lower than the conductivity of some linear PBI/PA adducts.[2–4] In fact, reported conductivities vary a lot and sometimes reach values close to these described in this work for the mesostructured composite (mp-PBI/PA-66). Some influence of the microstructure has already been suspected to explain the scatter of the conductivity data,[12] and it could well be that linear PBI/PA adducts may show some phase separation which is not expected for less flexible crosslinked PBI/PA adducts reported in this work. Unfortunately, no microstructural information is available on linear PBI/PA adducts so far.

Mesoporous PBI can be produced with varying amounts of crosslinker,[10] yielding mesoporous PBIs of varying flexibility. To investigate the influence of the flexibility of the pore walls, proton conductivities of PA doped mesoporous PBIs prepared with 10–40 mol % crosslinker were investigated. These measurements were performed at a doping level of 66 wt % PA and subsequent annealing for 12 h at 180 °C. Figure 4 and Table 1 show the results of conductivity measurements of samples with crosslinker contents varying from 10 to 40 mol %.

Crosslinker concentrations of 10 and 20 mol % resulted in the highest conductivity; otherwise the conductivity decreases with increasing concentration of crosslinker. Some crosslinking is actually required to preserve the porosity after leaching out

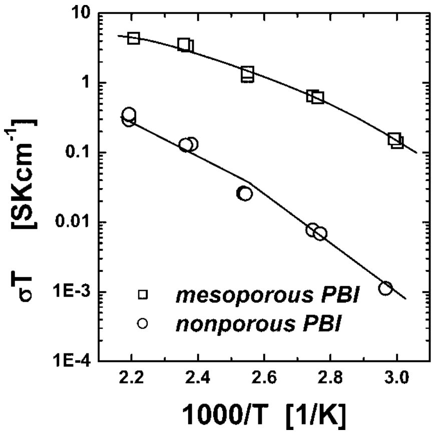

Figure 3. Plot of the proton conductivities of compressed pellets made of adducts of PA with mesoporous and nonporous PBI (PA content of each sample 66 wt %).

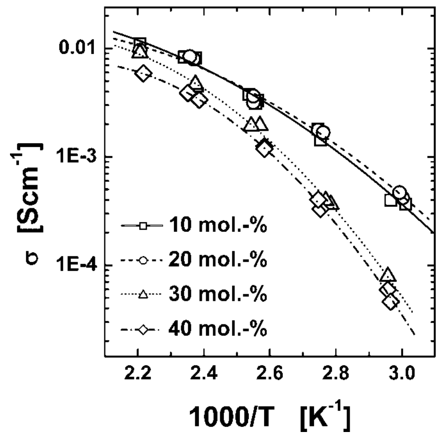

Figure 4. Plot of the proton conductivities of PA doped mesoporous PBI with varying crosslinker content; doping level 66 wt % PA; measurements were performed in closed cells.

Table 1. Proton conductivities of PA doped mesoporous PBI with varying cross-linker content; doping level 66 wt % PA; measurements were performed in closed cells.

Temperature [°C]	$\sigma_{10\ \mathrm{mol}\ \%}$ [mS cm^{-1}]	$\sigma_{20\ \mathrm{mol}\ \%}$ [mS cm^{-1}]	$\sigma_{30\ \mathrm{mol}\ \%}$ [mS cm^{-1}]	$\sigma_{40\ \mathrm{mol}\ \%}$ [mS cm^{-1}]
65	0.4	0.4	0.08	0.05
90	1.8	1.7	0.4	0.4
120	3.2	3.6	1.9	1.2
150	8.2	8.4	4.6	3.4
180	11.1	9.6	9.0	7.1

the quasi-spherical silica templates; too high levels of cross-linkers may limit the formation of connections between pores in the leaching process and in the filling with PA. As pointed out above, a well-connected pore structure is essential for obtaining high proton conductivity. This obviously forms at intermediate concentrations of crosslinker (10–20 mol %), at which pores are sufficiently stabilized but still can connect in the preparation process.

In conclusion, it was shown that the proton conductivity of the system PBI/PA benefits from the presence of a two-phase structure, that is, the development of a well-connected PA-rich domain leads to overall conductivities higher than those observed for "homogeneous" samples. Such structures may be obtained by filling mesoporous PBI with PA. The loading occurs in two steps: a fast step during which the mesopores are filled with molten PA and a second slower step, which leads to the incorporation of PA into the pore walls. The driving force of the first step is capillarity, and salt formation (acid/base reaction) is the driving force of the second reaction. If the initial volume of PA exactly matches the pore volume, this results in partial pore emptying and decreased proton conductivity. An excess amount of PA however, results in very good conductivities as both the mesopores and the pore walls are filled with PA. The optimum microstructure, at which pores are sufficiently stabilized but still connect in the preparation process, is found to form for an optimum concentration of crosslinker (10–20 mol %).

Nevertheless, the introduction of a defined nanostructure into crosslinked PBI/PA composites is a very promising approach towards improved high-temperature membranes for fuel cell applications. Currently, there are many attempts to improve the poor mechanical properties of PBI/PA membranes with high PA content, for example, by crosslinking the PBI matrix. Such approaches generally lead to some compromise between conductivity and mechanical properties. As suggested above, crosslinking may suppress phase separation, which is essential for obtaining high conductivity. The approach suggested in this work, however, provides the possibility to control the microstructure of crosslinked PBI. In such a way high proton conductivity and good mechanical properties are combined in a unique way.

Experimental

Synthesis: The synthesis of the mesoporous PBI has been described elsewhere [10]. The nonporous PBI was synthesized from diphenyl isophthalate, 1,3,5-triphenyl mesitylate, and 3,3′-diaminobenzidine by melt polycondensation following the protocol described in the literature [13].

Methods: The polymers were ball-milled to a fine powder. The powders were mixed with the specified amount of crystalline, anhydrous phosphoric acid in a glove-box under a dry argon-atmosphere. The composite material was placed in a glass tube of 6 mm diameter, contacted with Pt-foils, and pressed to a pellet. The closed cell was transferred to a hot oven (100 °C), and annealed at 180 °C overnight.

The resistance of the pellets was measured with ac-impedance spectroscopy using a 4192A LF machine from Hewlett–Packard. The conductivity could be calculated easily because the pellets had a well-defined geometry of 6 mm diameter and typical heights of 1 to 1.5 mm.

Nitrogen sorption measurements were performed at 77 K using a Quadrasorb machine from Quantachrome Instruments. SAXS measurements were performed under vacuum using a Kratky camera (slit focus) from Anton Paar instruments. The scattering vector s is defined as $s = 2\lambda^{-1}\sin\theta$, where λ is the wavelength of the X-rays (0.154 nm).

Received: December 19, 2007
Revised: January 28, 2008

---

[1] R. Bouchet, E. Siebert, *Solid State Ionics* **1999**, *118*, 287.
[2] Q. Li, R. He, J. O. Jensen, N. J. Bjerrum, *Fuel Cells* **2004**, *4*, 147.
[3] Y. L. Ma, J. S. Wainright, M. H. Litt, R. F. Savinell, *J. Electrochem. Soc.* **2004**, *151*, A8.
[4] J. S. Wainright, J. T. Wang, D. Weng, R. F. Savinell, M. Litt, *J. Electrochem. Soc.* **1995**, *142*, L121.
[5] T. Dippel, K. D. Kreuer, J. C. Lassegues, D. Rodriguez, *Solid State Ionics* **1993**, *61*, 41.
[6] A. Bozkurt, M. Ise, K. D. Kreuer, W. H. Meyer, G. Wegner, *Solid State Ionics* **1999**, *125*, 225.
[7] K. D. Kreuer, *J. Membr. Sci.* **2001**, *185*, 29.
[8] R. H. He, Q. F. Li, G. Xiao, N. J. Bjerrum, *J. Membr. Sci.* **2003**, *226*, 169.
[9] D. Mecerreyes, H. Grande, O. Miguel, E. Ochoteco, R. Marcilla, I. Cantero, *Chem. Mater.* **2004**, *16*, 604.
[10] J. Weber, M. Antonietti, A. Thomas, *Macromolecules* **2007**, *40*, 1299.
[11] H. Steininger, M. Schuster, K. D. Kreuer, A. Kaltbeitzel, B. Bingöl, W. H. Meyer, S. Schauff, G. Brunklaus, J. Maier, H. W. Spiess, *Phys. Chem. Chem. Phys.* **2007**, *9*, 1764.
[12] J. R. P. Jayakody, S. H. Chung, L. Durantino, H. Zhang, L. Xiao, B. C. Benicewicz, S. G. Greenbaum, *J. Electrochem. Soc.* **2007**, *154*, B242.
[13] H. Vogel, C. S. Marvel, *J. Polym. Sci. A* **1961**, *50*, 511.